Transport, magnetic, and optical properties of electrochemically doped poly(1,4-dimethoxy phenylene vinylene)

J. B. Schlenoff,* J. Obrzut, and F. E. Karasz
Department of Polymer Science and Engineering, University of Massachusetts, Amherst, Massachusetts 01003
(Received 10 July 1989)

A coordinated study on electrochemical, magnetic, optical, and transport properties of poly(1,4-dimethoxy phenylene vinylene) (PDMPV) using *in situ* electrochemical doping techniques is presented. Properties are correlated through a common axis of applied voltage. Electrochemical doping shows $\approx 100\%$ Coulombic efficiency up to an applied potential of 3.8 V versus lithium in propylene carbonate electrolyte. Conductivity increases in a reversible manner to a maximum of 250 $\Omega^{-1}\,\mathrm{cm}^{-1}$ and an applied potential of 3.9 V. Potentials in excess of 3.9 V cause an irreversible decrease in conductivity. Spin and charge show a 1:1 relation only to very low doping levels. Two paramagnetic species are produced on doping. A maximum spin concentration is observed at ≈ 3.7 V. The ultraviolet–visible–near-infrared spectra of doped PDMPV show at least five absorption bands, at 4.8, 3.7, 2.5, 1.7, and 0.6 eV. The first three bands decrease with doping and the latter two increase. When analyzed by the polaron or bipolaron model, the optical data imply significant symmetry breaking. Contributions to the optical activity from polarons and bipolarons are determined from the EPR results and are found to be different for both peaks, implying greater symmetry-breaking effects for polarons. An electrochemical analysis of EPR results suggests that polaron interaction energies are ≈ 0.45 eV greater than those for bipolarons.

I. INTRODUCTION

Numerous organic polymers containing an extensively π-conjugated backbone have been synthesized and doped, by partial oxidation or reduction, to yield materials with high electrical conductivity.[1,2] The nature of the electrical charge carriers that result from doping has been studied by magnetic[3,4] and optical[5,6] spectroscopy and by measurements on conductivity as a function of temperature[7] and doping level.[8] The resulting wealth of information on these conducting polymers allows the following qualitative conclusions to be drawn: (i) Doping dramatically increases conductivity (up to a point), (ii) conductivity decreases with decreasing temperature (the dependence is often seen to be a function of $t^{1/4}$, indicative of variable-range hopping), and (iii) chromophores due to electronic transitions are generated upon doping which have absorbance energies lower than the absorption usually associated with the interband transition. Doping often produces paramagnetism, typically studied with EPR to observe unpaired spins, though the overall picture is less clear. Conducting polymers show either a constant concentration of spins with doping,[3,9] a decrease of spin concentration,[8,10] an increase,[11] a maximum,[12] or two maxima.[13] That strongly contrasting behavior has been obtained from the same polymer[14,15] is symptomatic of a general inconsistency in EPR results. However, the observation of doping-induced spin susceptibility at some point in the doping seems to be general. Both spin populations and dynamics, and electrical conductivity are sensitive functions of impurities and defects introduced during synthesis and sample handling. Exposure to oxygen, for example, has marked effects on both of these parameters.[16] Optical spectroscopy, on the other hand, appears to be more robust with respect to small concentrations of impurities and there is general consensus on optical behavior for a particular polymer.

Interpretation of the properties of conducting polymers with nondegenerate ground states is popularly done with the polaron and bipolaron model.[17,18] Both are localized states which have two levels positioned symmetrically about midgap between conduction and valence band. Distinction between these two types of defect by optical-absorption spectroscopy is often rendered inconclusive by the breadth of the absorption bands and possible interactions. Thus EPR may be used to discriminate between polarons and bipolarons, since the former have spin $\frac{1}{2}$ and the latter have spin 0. If the number of spins produced as a result of electrochemical doping is less than the number of charges injected then a distribution between polaron and bipolaron states is said to exist.[12]

Although one of the prime motivations for studying the properties of conducting polymers is to determine the mechanism of their electrical conductivity, little work has been done on actually determining the conductivity as a function of doping level for electrochemically doped polymers.[3,19] Species detected by spectroscopic means are often referred to as "charge carriers," implying that all spectroscopically active species contribute to electrical conductivity. Thus the main focus of the present work is in correlating changes in conductivity to regions of doping (i.e., electrochemical activity) and to regions of spectroscopic activity. For this work we sought to identity a well-characterized polymer for a series of coordinated experiments on the dependence on doping of optical, magnetic, electrochemical, and electrical transport properties. The phenylene vinylene class of conducting polymers represents a particularly versatile selection of materials for this purpose.[20–22] These polymers are synthesized from processible, water-soluble precursor

polyelectrolytes. They have several advantages over the electrochemically prepared polymers, such as polypyrrole,[23], polythiophene,[24] and polyaniline,[25] that are usually employed for *in situ* optical and magnetic studies. Polyphenylene vinylenes are partially crystalline and may be stretch oriented to increase order.[26] Structural parameters can be determined[27] which are valuable for theoretical calculations requiring bond angles and lengths[28] (electropolymerized conducting polymers are, in contrast, amorphous). Furthermore, phenylene vinylene polymers are prepared with high molecular weight ($M_n > 100\,000$) which minimizes effects due to chain ends. These polymers can also be purified, blended,[29] and copolymerized.[30] For the present work we chose poly(1,4-dimethoxy phenylene vinylene) (PDMPV), structure I,[31] over the parent poly(*p*-phenylene vinylene) (PPV), structure II, because the former possesses additional advantages with regard to electrochemical properties:[32] a lower oxidation potential than that of PPV (Ref. 33) allows the polymer to be cycled with high Coulombic efficiency, and PDMPV exhibits superior ionic conductivity, allowing films several micrometers thick to be charged or discharged.

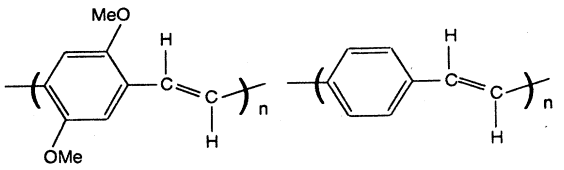

I II

Electrochemical doping, as opposed to chemical doping, has become the preferred technique for the doping of conducting polymers[34,35] since it can be reversible, controlled, homogeneous, precise, and reproducible.[3,36,37] Further, electrochemical doping may be performed *in situ* in combination with other techniques, avoiding problems due to sample handling and transfer, and improving precision. With this judicious choice of material and doping technique we provide a coherent set of data on some of the most widely-studied physical properties of conductive polymers. We then analyze the observed experimental results using a small sampling of some of the extensive theoretical work on the novel solid-state physics of these low-dimensional conductors.

II. EXPERIMENTAL TECHNIQUES

A. Materials

A ≈ 0.2 wt. % aqueous solution of the water-soluble tetrahydrothiophene precursor to PDMPV was synthesized according to previously described procedures.[31] Films of precursor, 3–4 μm in thickness, for EPR and conductivity measurements were cast under vacuum onto silanized optically flat glass. For the ultraviolet–visible–near-infrared spectrophotometry films 0.1–1 μm thick were cast under flowing argon onto 100 lines-per-inch platinum mesh. Precursor conversion to PDMPV was accomplished by a final thermal elimination carried out at 200 °C for 4 h under a dynamic vacuum of $< 10^{-4}$ Torr. Efficient conversion to structure I was indicated by an absence of tetrahydrothiophene, determined by elemental analysis for sulfur. Electrolytes were either 1*M* $LiClO_4$ (Aldrich, dried under vacuum at 180 °C) or 1*M* $LiAsF_6$ (USS Agrichemicals) in propylene carbonate (Burdick and Jackson). Counter and reference electrodes were 0.7-mm lithium ribbon (Alpha Ventron). All potentials are referenced to the Li/Li^+ (1*M*) couple.

B. EPR

PDMPV samples for *in situ* EPR and electrochemistry were sputtered on one side with 20 nm of platinum to ensure homogeneous current distribution across the film. A weighed sample of approximately 50 μg of polymer, ≈ 3 μm thick, was attached to 0.1-mm Pt wire and inserted into a standard quartz EPR flat cell filled with 1*M* $LiClO_4$/propylene carbonate electrolyte. A small piece of lithium ribbon attached to 0.1-mm nickel wire was then inserted into the flat cell above the polymer and the cell was sealed off with hard wax. All cell assembly was performed in an argon-filled dry box. The cell was placed in the resonance cavity of an IBM ESR300 spectrometer and its position optimized with the aid of a small, weighed crystal of 1,1-diphenyl-picrylhydrazyl (DPPH) taped to the outside of the cell next to the sample. The DPPH also served as a standard for the determination of absolute spin susceptibility. Electrochemical doping was controlled with a Princeton Applied Research (PAR) 173 (179) potentiostat coulometer or a PAR 273 potentiostat. Simultaneous EPR and cyclic voltammetry was achieved by overmodulating the magnetic field (20 G modulation amplitude), setting the spectrometer to the peak maximum and scanning the voltage while recording the current-voltage characteristics on an *X-Y* recorder. This technique gives a peak height that is proportional to the spin concentration regardless of small changes in peak shape due to intrinsic changes in line shape or broadening due to unresolved peaks (the linewidth is governed by the amplitude of the modulation).[13] Unpaired spin concentrations were obtained by double integration of the signal and comparison to the DPPH standard, or by comparison of the intensity of the overmodulated sample to that of the standard. Both methods gave the same results. For saturation studies the *in situ* cell could not be used, owing to excessive absorption by the polar electrolyte. Thus, saturation studies were done on samples doped in the dry box, dabbed dry, inserted into 3- mm quartz tubes and sealed.

C. Electrical conductivity

A piece of PDMPV, ≈ 1 mm $\times 3$ μm $\times 8$ mm, was typically inserted into a doping cell constructed from a $\frac{1}{2}$-in.-i.d. Teflon vacuum stopcock. This cell had four coplanar, parallel Pt wires, 0.1 mm in diameter, spaced 1 mm apart, which fed through holes drilled into a $\frac{1}{2}$-in.-diam medium porosity glass frit. Pressure to the film was applied via the stopcock, ensuring good electrical contact. Access of electrolyte to the film was through the

frit. The PDMPV was doped to the desired level by shorting the four leads together and slowly scanning to the appropriate potential. After the current had dropped to a low value (typically ≈ 0.2 μA), indicating an approach to doping equilibrium, the PAR 173 was reconfigured to provide a constant potential of 1–10 mV across the outer two leads and the potential across the inner leads was measured with a Keithley 617 electrometer. The current was obtained from the PAR 173 and was used to determine the four-probe conductivity. The importance of applying a low potential (<10 mV) between the two outer electrodes should be noted, since a large voltage gradient across the film will lead to a gradient in doping level.[37]

D. Ultraviolet–visible–near-infrared

An electrochemical cell was constructed in the dry box using a 1-cm pathlength quartz cuvette. PDMPV on Pt mesh, lithium counter, and reference electrodes were positioned inside the cuvette. The cell was filled with 1*M* $LiAsF_6$/propylene carbonate and was sealed with silicone rubber. A Perkin Elmer Lambda 9 spectrophotometer was used to record absorption spectra from 185 to 2500 nm while the polymer was electrochemically doped using the PAR 273. The potential was either stepped to a specific value and the entire spectrum recorded or the monochromator was set to a peak maximum and the voltage scanned.

E. Fourier transform infrared spectroscopy (FTIR)

A Mattson Cygnus 100 FTIR was used to recored ir spectra with 2 cm^{-1} resolution. Samples were either pristine or were subjected to doping or undoping cycles in the dry box using a doping cell similar to that used for conductivity measurements, which allowed pressed contact of platinum foil to polymer.[3]

III. RESULTS

A. Electrochemical behavior

PDMPV may be cycled with $>98\%$ Coulombic efficiency between 2.5 and 3.8 V versus Li/Li^+ in the electrolytes studied. This high efficiency permits accurate calculation of the doping level from the amount of charge passed. Other conducting polymers with higher oxidation potentials, such as PPV (Ref. 38) and polyacetylene,[34] suffer from parasitic side reactions during charging, such as the oxidation of propylene carbonate,[39] especially at the higher doping levels. Two oxidation reactions and two reductions are seen when cycling to 3.8 V (Fig. 1). Oxidation is chemically reversible up to a potential of about 3.9 V—the polymer is stable to repeated cycling up to this potential. Voltammograms using the $LiClO_4$ and $LiAsF_6$ electrolytes were identical. Figure 2 shows the dependence of doping level on potential for charging and discharging. Although the doping current continues to rise past 3.8 V, efficiency starts to decrease and the doping level becomes less precisely known. At potentials higher than ≈ 3.9 V irreversible oxidation occurs and voltammograms become irreproducible. Such regimes of initial reversibility followed by irreversibility at higher potentials is behavior generally observed in conducting polymers (for example in polyacetylene,[40] polyaniline,[41] and polypyrrole[42]).

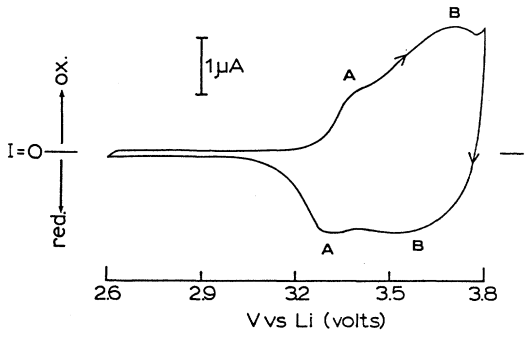

FIG. 1. Cyclic voltammogram of PDMPV in propylene carbonate/1*M* $LiClO_4$. Scan rate, 0.2 mV sec^{-1}. Peak assignments are described in text.

B. Electrical conductivity

The *in situ* conductivity is shown as a function of potential in Figs. 3 and 4. Two consecutive cycles to 3.8 V are given in Fig. 3, which indicate the reversibility of conductivity behavior to this limit of applied potential. The conductivity samples were cycled over the same time scale (≈ 4 h) as the cyclic voltammetry or EPR samples

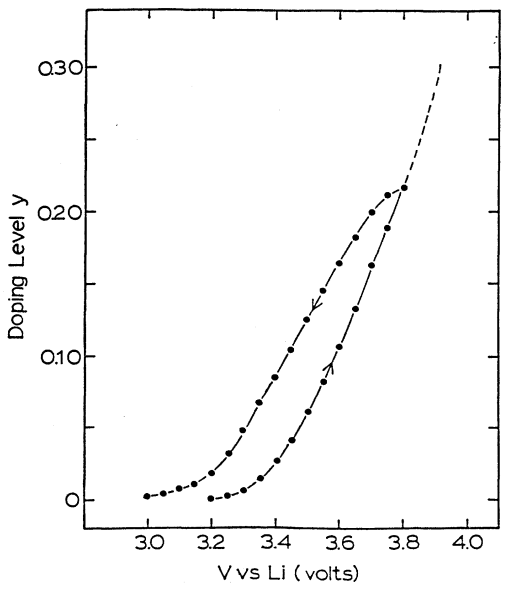

FIG. 2. Doping level of PDMPV as a function of applied potential for charging and discharging. The dashed line represents continued charging past 3.8 V.

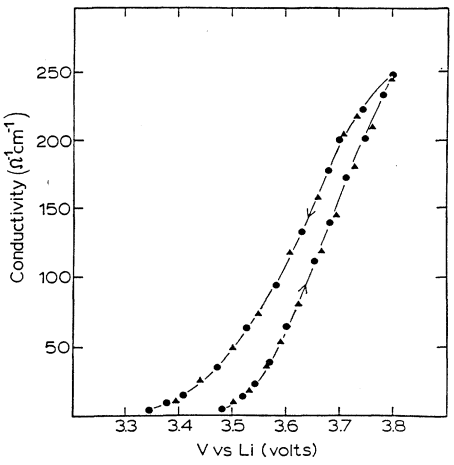

FIG. 3. Reversible *in situ* conductivity for 3-μm-thick PDMPV vs *V*. Two consecutive cycles are shown (circles and triangles).

to allow correlation between data. The maximum conductivity reached was 260 $\Omega^{-1}\,\mathrm{cm}^{-1}$ and the minimum measured conductivity, limited by the ionic conductivity of the electrolyte, was $\approx 2\ \Omega^{-1}\,\mathrm{cm}^{-1}$. A similar *in situ* four-probe arrangement, on a much smaller scale, was employed by Wrighton[37] to demonstrate an electrochemical "transistor" based on polypyrrole. Exposure of PDMPV to greater than 3.9 V led to an irreversible *decrease* in conductivity, as shown in Fig. 4. This is also a general feature in conducting polymers (for example, polyacetylene,[43] polyaniline,[44] and polypyrrole[37]).

C. EPR

Nascent PDMPV was completely devoid of paramagnetic susceptibility within the detection limit of the technique used (1 spin per 10^4 monomer repeat units, or 1 spin per 10^5 carbons). The spin concentration showed complex behavior with applied potential, which depended on the voltage limit of the doping cycle. Films doped to an upper limit of 3.7 V could be undoped back to a zero-spin-concentration state. Figure 5 shows consecutive scans, taken at 0.2 and 0.05 mV sec^{-1}. A steady increase in spin density with potential is seen followed by a return to baseline on sweep reversal. Decreasing the scan rate by a factor of 4 is seen to decrease the small hysteresis between doping and undoping. This hysteresis is due to positive or negative overpotential required to drive the sluggish interfacial charge transfer to the polymer. It is not a result of slow diffusion of counter ions (perchlorate) during the doping, since the two scan rates lead to nearly identical spin concentration versus potential profiles. It is important to note that the number of spins introduced was usually less than the charge injected. This is clearly demonstrated in Fig. 6, where the spin concentration as a result of constant-current doping is shown. The sample in Fig. 6 was doped at a constant current of 0.016 mA mg^{-1} to a final potential of 3.60 V and a doping level of 2.8%, i.e., $[C_{10}H_{10}O_2(ClO_4)_{0.028}]_n$. The response for a theoretical 1:1 spin to charge ratio is shown as the dashed line in Fig. 6. Only at the very beginning of the cycle, up to an applied potential of 3.45 V, and a doping level of $<0.5\%$, does the spin density equal the charge density. A similar result was seen for the electrochemical *p*-type doping of polypyrrole.[12]

For potentials of up to 3.7 V a single, narrow ($\Delta H_{pp} \sim 0.5$ G, $T_2 \sim 130$ ns) line is seen, *g* value 2.0030. This signal can be homogeneously saturated as shown in Fig. 7; T_1 is 8.3 μsec from this plot. If the potential is increased to higher than 3.7 V, the dependence of spin con-

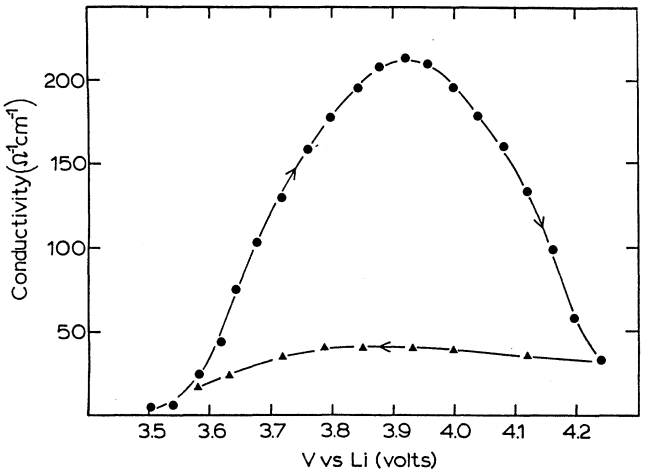

FIG. 4. Irreversible conductivity change as a function of applied potential for charging (circles) followed by discharging (triangles) at ≈ 0.2 mV sec^{-1}.

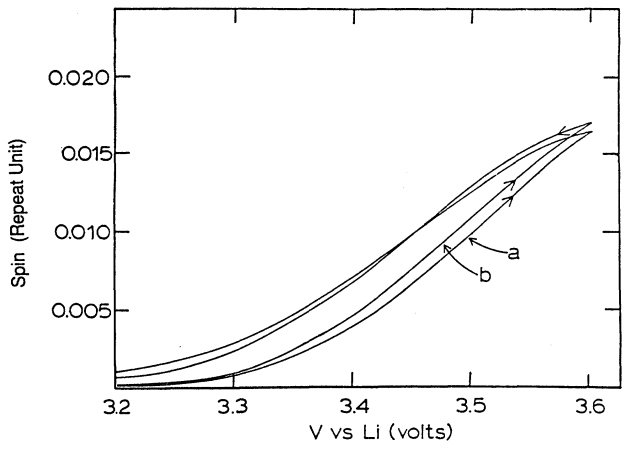

FIG. 5. Spin concentration vs applied potential for scanning at 0.2 mV sec^{-1}, *a*; and 0.05 mV sec^{-1}, *b*.

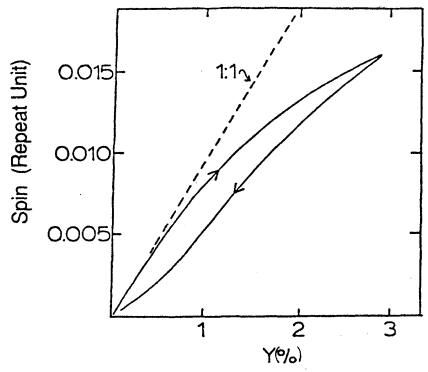

FIG. 6. Spin concentration as a function of doping level for constant-current doping at PDMPV at 0.016 mA mg^{-1}. The dashed line represents theoretical response for one spin per injected charge.

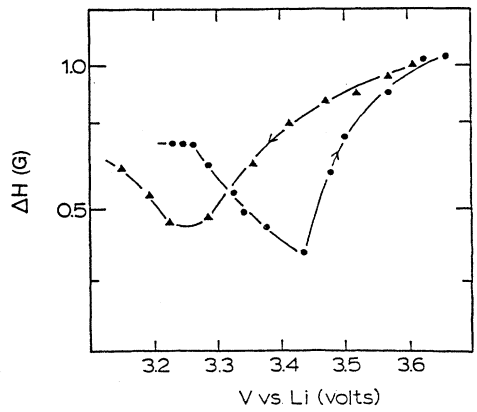

FIG. 9. Peak-to-peak linewidth vs potential of EPR signal for *in situ* doping (circles) and undoping (triangles) of PDMPV.

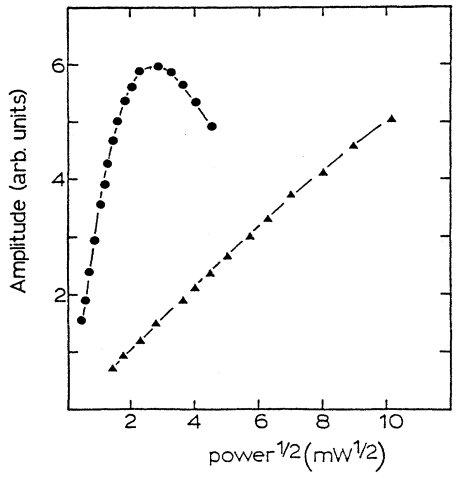

FIG. 7. EPR saturation plot of PDMPV doped to $y=0.02$ and 0.14.

centration on voltage changes. A peak in the cyclic voltammetry is developed at about 3.4 V and a shoulder appears in the spin concentration versus V at the same potential (Fig. 8). The spin concentration can be decreased with undoping but does not return to zero. Two components are now seen between 3.2 and 3.7 V, as suggested by the plot of linewidth versus potential in Fig. 9; the linewidth decreases with doping up to a potential of 3.45 V, consistent with a narrowing mechanism due to spin exchange.[13] The line then rapidly broadens as another component with almost the same g value is introduced. For the *in situ* samples the slight difference in g values causes the line to be asymmetric, though the components are unresolved. If the sample is then removed and pumped dry the narrow component becomes still sharper and the two components can be seen (Fig. 10). The presumption was that if narrowing were due to spin ex-

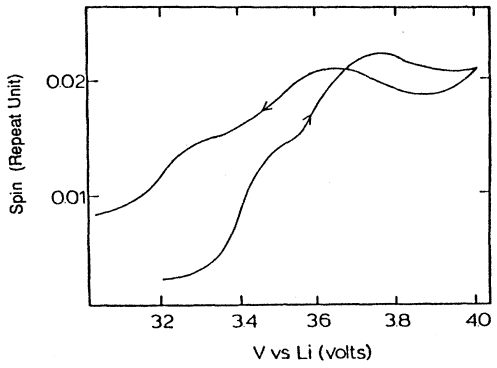

FIG. 8. Response of spin concentration upon scanning applied potential at 0.2 mV sec^{-1}.

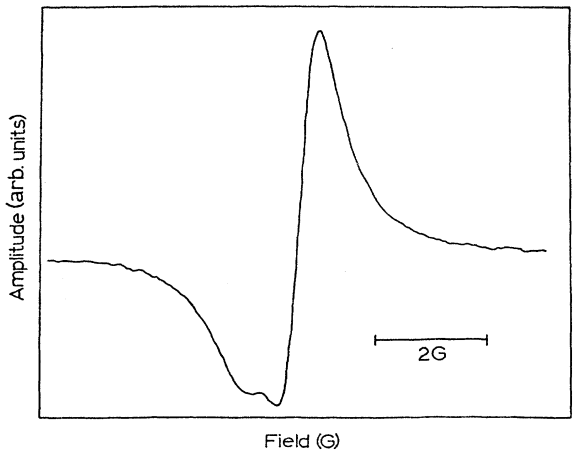

FIG. 10. EPR signal at PDMPV doped to $y=0.12$. The sample has been removed from solvent and pumped dry to show two components.

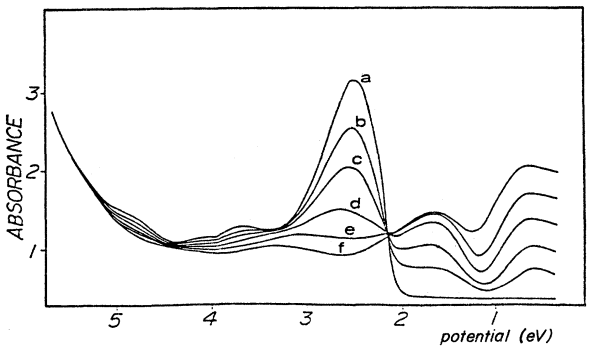

FIG. 11. Electron absorption of PDMPV from 0.4 to 5.7 eV recorded *in situ* on doping to 2.6, *a*; 3.4, *b*; 3.45, *c*; 3.55, *d*; 3.65, *e*; and 3.8 V, *f*.

change the removal of swelling solvent[45] would increase the spin density and the line would become further narrowed. The broad component could not be saturated. The spin concentration shows a *maximum* at ~3.8 V when scanning to 4.0 V, as seen in Fig. 8. Scanning to 4.3 V reveals another maximum, although the repeatability of cycles at these higher potentials is poor.

D. Electronic spectra

The electronic absorption spectrum of undoped PDMPV recorded from 0.4 to 5.7 eV is shown in Fig. 11. Spectra taken after stepping to increasing doping potentials are also shown. The large band at 2.5 eV and small-

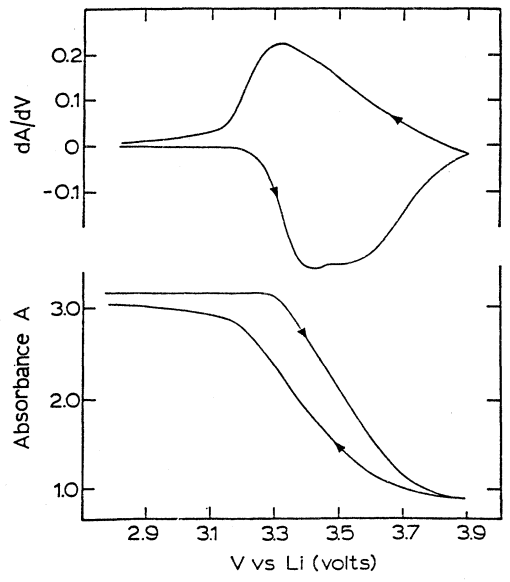

FIG. 12. Absorbance and derivative of absorbance of peak at 2.51 eV as a function of applied potential, for PDMPV, 160 mm thick, cycled at 5 mV sec^{-1}.

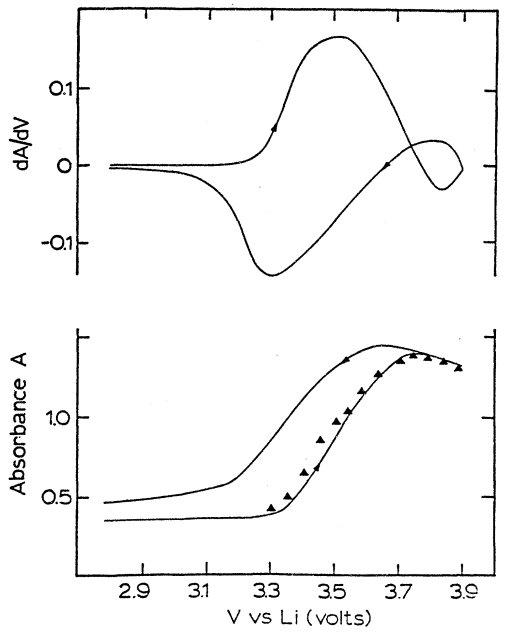

FIG. 13. Absorbance and derivative of absorbance of peak at 1.68 eV as a function of applied potential, for PDMPV, 160 mm thick, cycled at 5 mV sec^{-1}. ▲, calculated fit using data from Fig. 16 and $\varepsilon_{pol}=4.6\times10^5$, $\varepsilon_{bipol}=0$.

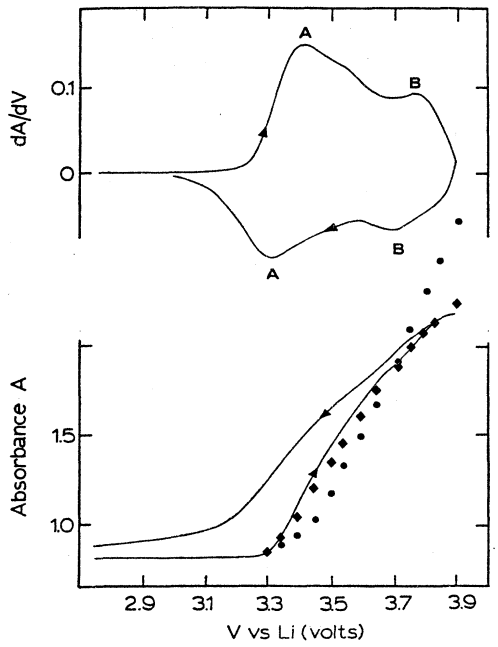

FIG. 14. Absorbance and derivative of absorbance of peak at 0.64 eV vs potential for PDMPV, 160 mm thick, cycled at 5 mV sec^{-1}. The peak assignments are described in text. ●, calculated fit using data from Fig. 16 and $\varepsilon_{pol}=0$, $\varepsilon_{bipol}=1.4\times10^5$; ◆, $\varepsilon_{pol}=2.6\times10^5$, $\varepsilon_{bipol}=6.4\times10^4$.

er ones at 3.7 and 4.8 eV decrease on doping and two peaks at 1.7 and 0.6 eV evolve. Figures 12–14 show the absorption, at fixed wavelength corresponding to the peak maxima at 2.51, 1.68, and 0.64 eV, plotted against voltage for a scan rate of 5 mV sec^{-1}. Figures 12 and 14 show the expected decrease and increase, respectively, of oscillator strength upon doping. The band at 1.68 eV, however, shows unexpected behavior, in that there is a maximum at about 3.8 V before the scan direction is switched. When compared to the cyclic voltammogram recorded simultaneously it is clear that optical density actually *decreases* from 3.6 to 3.9 V while the polymer is still acquiring charge over the same range.

IV. DISCUSSION OF RESULTS

A. Reversible and irreversible electrochemical doping: generation of charge carriers

The partial oxidation of PDMPV occurs in many steps, since a peak or shoulder in the cyclic voltammetry represents the transfer of one or more electrons. Over the range of potential studied the electronic conductivity only increases up to a potential of 3.9 V and a doping level of 32%. This range encompasses two pairs of oxidation reductions in the cyclic voltammetry, suggesting that at least two species exist over the range where the conductivity is reversibly controlled by doping The cyclic voltammetry of most conductive polymers shows at least two reversible peaks or shoulders.[1] At higher applied potentials a significant, irreversible decrease in conductivity is observed (Fig. 4). It should be noted that a wide range of conductivity ($\sim 10^{-12}$–1 $\Omega^{-1}\,cm^{-1}$), is not accessible using the *in situ* technique here because of the limitation imposed by the parallel conductivity of the electrolyte. Thus the measured conductivity starts to increase at higher potentials.

In a recent study on the x-ray photoelectron spectra of neutral and doped PPV it was noted that a high-binding-energy component of the C (1*s*) peak appeared on doping, which was attributed to a local nonequivalence of electron densities on the carbon atoms.[46] Our premise is that doping produces localized, charged states which serve as centers to which electronic charges can hop to and from. In the Mott formalism, conductivity is due to hopping in a manifold of states at the Fermi level,[47,48] in this case hole states. These states are, chemically speaking, carbocations delocalized over about three monomer repeat units. When an electron hops to a hole the charge will be neutralized. There will thus be a steady-state population of both holes and neutral sites on the polymer backbone.[49] This requirement for a *mixture* of neutral and positive sites is met over most of the doping range. If an excess of positive charges is introduced—if the polymer is "overdoped"—the conductivity will decrease, since the requirement for a mixture of states is not met. Thus, there is a "window" of high conductivity, as is also seen for polyaniline (PAn).[44] In contrast to PAn, the PDMPV doping at higher potentials appears to be chemically irreversible (Fig. 4). The hopping frequency and thus the electrical conductivity depend on the energy barrier for charge transfer between sites. Studies on the temperature dependence of the conductivity of PPV, performed over the range 4–300 K suggest that hopping occurs in three dimensions.[50] The hopping probability for three-dimensional variable-range hopping will increase as the charge density increases (within the requirements for a mixture of sites), and may also be enhanced by screening of charges by dopant ions (counter ions).

The FTIR spectra for doped and undoped PDMPV, shown in Figure 15, and nascent PDMPV (not shown) are identical except for an additional small peak at 1800 cm^{-1} (due to $\approx$0.5 wt.% of residual propylene carbonate) in the cycled PDMPV. An important conclusion is that PDMPV retains its chemical integrity even on cycling to potentials above 3.8 V. Of particular noteworthiness is the absence of degradation in the 1200–1300 cm^{-1} range, which encompasses the vibrational bands due to —O—CH_3. These aromatic methoxy groups thus appear to be more oxidatively stable than aliphatic ethers, which tend to oxidize above 3.5 V. Also evident in Fig. 15 is a lack of activity at 580 cm^{-1} due to ClO_4^- ion (a band which is clearly evident in slightly doped samples). The polymer can thus be completely undoped. Although no evidence of structural degradation is seen from the Fourier-transform infrared (FTIR) spectra, films cycled to potentials >3.9 V were considerably more fragile and brittle than those kept below this limit. It is quite possible that doping at high potentials causes chain scission, introducing a few percent of saturated (sp^3) carbons which are not discernible by FTIR but which significantly reduce conductivity. The very strong effect that defects of this type have on conductivity has been noted for polyacetylene and polyparaphenylene.[51,52] Although early experiments on PPV in a powder morphology[53] seemed to confirm theoretical arguments that a copolymer should have a lower conductivity than a homopolymer[54]—PPV can be thought of as an alternating copolymer of polyacetylene and polyphenylene—PPV films prepared from the precursor method can be doped to conductivities three orders of magnitude higher than powder samples.[32]

B. Electronic excitations. polaron-bipolaron model

In situ optoelectrochemistry of conducting polymers with nondegenerate ground states is usually interpreted in terms of the polaron-bipolaron model as introduced by Brazovskii and Kirova (BK),[54] who extended the continuum limit[55] of the degenerate ground-state model of Su, Schrieffer, and Heeger (SSH),[56] to nondegenerate polymers. As a result of electron-phonon coupling and lattice distortion two localized electronic states appear in the gap between conduction and valence bands positioned symmetrically about midgap.

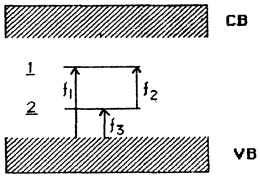

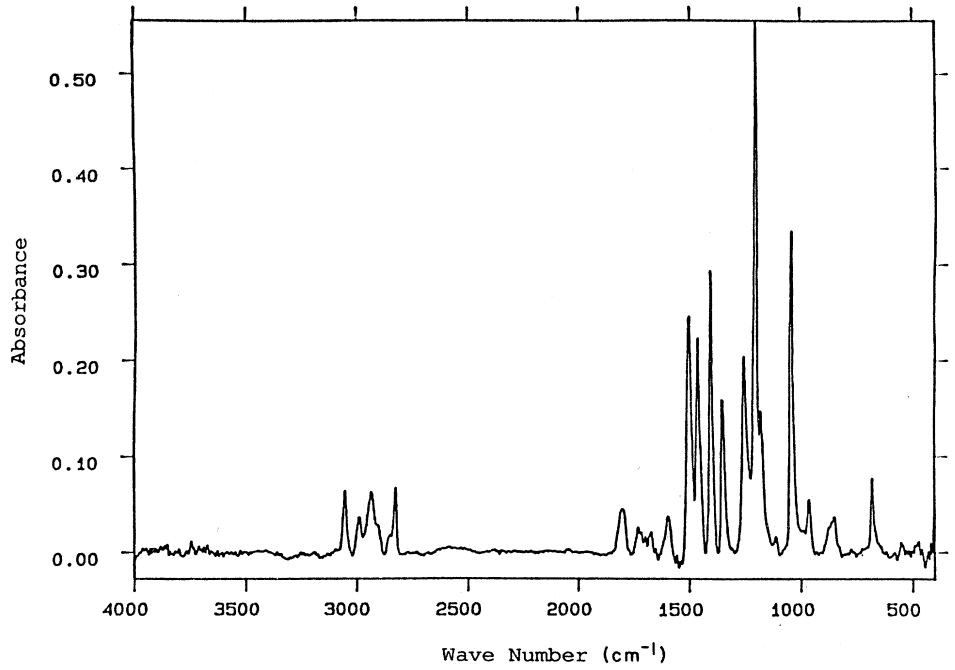

FIG. 15. FTIR spectrum, from 400 to 4000 cm^{-1}, of PDMPV, 3 μm thick, doped to 4.1 V and undoped to 2.6 V in 1M $LiClO_4$/propylene carbonate.

For hole polarons, the lower level, 2, is singly occupied, and for hole bipolarons both subgap levels are empty, and the defect is doubly charged and spinless. These polarons and bipolarons are thus radical cations and spinless cations within the boundaries of the electron-phonon lattice distortion band model. Electronic transitions are possible from the valence band (VB) to both levels for bipolarons (f_1 and f_3) and there is an additional transition between the localized states for a polaron (f_2) since the lower state is occupied.

Although doping past 3.9 V produces additional optical density this absorption is irreversible and is associated with species that do not give rise to conductivity. Thus only the region between 3.0 and 3.8 V will be considered in detail.

The general features of the optical spectroscopy in Fig. 11 are readily interpreted by the polaron-bipolaron theory. The undoped polymer shows an absorption edge at 611 nm (the band gap is thus 2.03 eV) with no absorption in regions of higher wavelength. The peak at 2.5 eV represents excitation from valence to conduction bands. As the polymer is doped, oscillator strength is removed from the interband absorption peak and two absorptions appear in the subgap region at 1.68 and 0.64 eV (738 and 1926 nm). Thus, with only two peaks apparent, at first it would seem that bipolarons are the species which result from doping. Indeed, the relationship

$$hf_1 + hf_3 = 2\Delta_0 , \tag{1}$$

where $2\Delta_0 = E_g$, the band gap, holds well in this case, demonstrating the electron-hole symmetry that is expected for bipolarons.[18] Although the optical spectroscopy appears to follow the prescribed behavior for bipolarons, including two peaks that adhere to electron-hole symmetry and a clear isosbestic point at about 2.1 eV, some aberrant behavior is seen when the amplitudes of the peak maxima at 2.51, 1.68, and 0.64 eV are followed as a function of applied potential, as in Figs. 12–14. Although the interband absorption shows the expected decrease with doping (Fig. 12), the peak at 1.68 eV actually decreases in intensity past 3.7 V in a region where both conductivity (Fig. 3) and doping level (Fig. 2) are still increasing. The first derivative of the absorption is nearly zero at the same point that a peak (at 3.6 V) occurs in the cyclic voltammetry. In addition, the maxima of the derivative of the absorption at 0.64 eV (Fig. 14) are opposite in relative magnitude to those for the cyclic voltammetry—the anodic peak at 3.3 V is larger than the peak at 3.6 V for the derivative of the absorption, whereas the situation is reversed for the voltammetry. Further evidence of the more complicated nature of the number and kind of defects involved in the doping of PDMPV is provided by the results of Sec. IV C on EPR, which demonstrate a coexistence of polarons and bipolarons over the potential range studied.

The shortcomings of a straightforward application of the bipolaron model to these data is further demonstrated by estimating the peak positions from the bandwidth. The interband absorption peak at 2.5 eV is much narrower than predicted by the bipolaron theory. To illustrate this, the model of Fesser *et al.*[57] is used to estimate

the confinement parameter β using the observed bandwidth W of 1.5 eV. β is given by $\beta=\Delta_e/\delta(\Delta_0+\Delta_e)$, where Δ_e is related to σ bonding and is estimated to be 1 eV and δ is calculated from $\Delta_0=W\exp(-1/\delta)$. A value for β of 0.15 is obtained which gives a ratio f_0/Δ_0 of 0.1 using Fig. 4 of Ref. 57. From this, two bipolaron levels $\Delta_0+f_0=1.1$ eV and $\Delta_0-f_0=0.9$ eV, are predicted, which are in disagreement with the experimental results. If the peak at 2.5 eV were broader the calculated bipolaron values would be closer to those observed.

The relative heights of the peaks are also inconsistent with the theory. In the treatment for a bipolaron the higher-energy subgap peak (HEP) at 1.68 eV should be considerably smaller than the lower-energy peak (LEP) at 0.64 eV, whereas they are actually almost identical in height (in the one-electron Hückel model the f_1 transition is symmetry forbidden[58]). This discrepancy has been recognized and attributed to the particularly high symmetry of the BK-SSH model.[59] Numerous approaches have thus been made to introduce symmetry-breaking parameters into the original SSH model. Couloumb interactions have been invoked[60,61] as have diatomic $A=B$-type polymers.[62] Sum *et al.*[59] introduced an electron-lattice coupling parameter, which is single-particle, short-range charge conjugation and "supersymmetry"-breaking contribution. The predicted results are a significant transfer of energy from the LEP to the HEP, asymmetry of peaks around the gap center, and a finite width for the bipolaron, as opposed to infinite in the Takayama–Lin-Lin–Maki (TLM) continuum model. Although the presence of asymmetry is not clear it is apparent that the bipolaron-polaron peaks are almost equal in height. Extensive breaking of symmetry can thus be inferred. Another effect of electron-lattice symmetry breaking is to cause the f_3 and f_2 polaron peaks to move together and coalesce. It thus becomes impossible to discern the existence of polarons and bipolarons simply on the basis of the number of observed electronic absorptions.

C. Discrimination between polarons and bipolarons: thermodynamics of charge carriers

Although the observed electronic absorption of PDMPV can be rationalized in terms of the TLM formalism, modified by electron-lattice or other symmetry-breaking coupling, the issue of whether the species present are polarons or bipolarons remains. Further, there is the question as to the source of the unusual behavior of the peak at 1.68 eV compared to the one at 0.64 eV. For the thermodynamic treatment that follows at least two assumptions are made: the two types of paramagnetic species are treated as one and the parameters recorded during charging may be correlated with the equilibrium values. The first assumption is necessary because there is no theory available to deal with two polarons simultaneously. The latter is justified since the hysteresis observed is due to charge transfer resistance at the polymer-solution interface and does not reflect a bulk concentration gradient (e.g., see Fig. 5). Effectively, a similar displacement (of 50–100 mV) of the recorded value from the zero-current value is seen for the y versus V data, and for the other parameters recorded as a function of V. Thus it is possible to correlate data recorded on charging or discharging cycles.

EPR provides a straightforward means of discriminating between polarons and bipolarons. With a knowledge of the number of polarons n_{pol} and the charge consumed in the reaction (doping level), Q, the bipolaron concentration n_{bipol} may be obtained,

$$Q=2n_{\text{bipol}}+n_{\text{pol}} . \tag{2}$$

This charge balance equation is only accurate if the charging is 100% efficient, which, for the present system, is a good assumption over the range to 3.8 V and less so up to 4.0 V (charging to 4.0 V is $\approx$83% efficient). The polaron and bipolaron populations, as a function of potential, are shown in Fig. 16 for a charging cycle. It is apparent that bipolarons rapidly become the dominant species as doping proceeds. It is also clear that the bipolaron concentration continues to increase after 3.7 V while the number of polarons *decreases* over the same range. By comparison with Fig. 3 it may be deduced that bipolarons definitely contribute to electrical conductivity and polarons probably contribute.

Since it is unlikely that two electrons will be removed simultaneously from a neutral site, two mechanisms can be given that produce bipolarons via polarons. The first possibility is electrochemical generation of two polarons, followed by chemical combination as follows:

$$x=p^{+\cdot}+e^- , \tag{3}$$

$$2p^{+\cdot}=(\text{bp})^{2+} . \tag{4}$$

The distribution of p and bp might be expected to show a

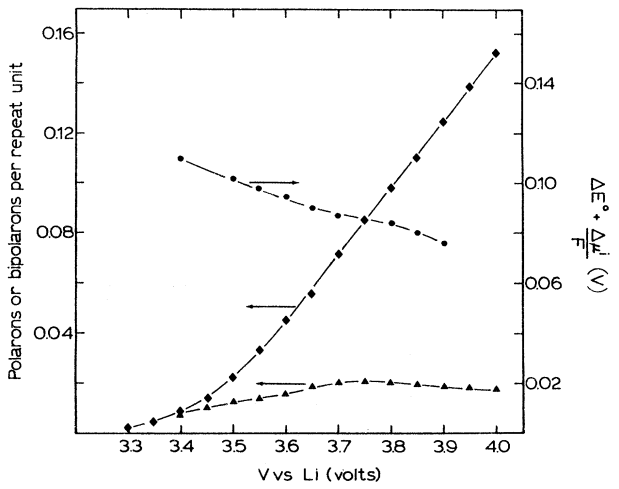

FIG. 16. Polaron, ▲, and bipolaron, ♦, populations, determined from coulometry and EPR, as a function of potential, ●. Difference between polaron and bipolaron standard formation potentials, E^0, plus difference in interaction potentials, as a function of V_{applied} for charging at 0.2 mV sec^{-1}.

second-order dependence on the concentration of polarons, e.g.,

$$K=\frac{[p]^2}{[\mathrm{bp}]} . \tag{5}$$

No satisfactory fit to this kind of behavior could be made with any value of K.

The second mechanism involves removal of two electrons sequentially in two electrochemical steps, as outlined by Nechstein *et al.* for polypyrrole,[12]

$$x \underset{E_p^0}{\overset{-e^-}{\rightleftarrows}} p^+ \underset{E_{\mathrm{bp}}^0}{\overset{-e^-}{\rightleftarrows}} [\mathrm{bp}]^{2+} , \tag{6}$$

where E_p^0 and E_{bp}^0 represent standard potentials for polaron and bipolaron formation, respectively, from a neutral site x. It is then assumed that the equilibrium concentrations are governed by the Nerst equation. Thus

$$\begin{aligned} E &= E_p^0+\frac{RT}{F}\ln\left[\frac{[p]}{x}\right]+\frac{\mu_p^i}{F} \\ &= E_{\mathrm{bp}}^0+\frac{RT}{F}\ln\left[\frac{[\mathrm{bp}]}{[p]}\right]+\frac{\mu_{\mathrm{bp}}^i}{F} , \end{aligned} \tag{7}$$

where x is the number of neutral sites. In this case the total number of sites is taken to be $y=0.32$, since this is the maximum doping level achieved before the doping becomes irreversible and the conductivity starts to degrade. There is some uncertainty in the exact value of this maximum doping level since the reversal in conductivity (Fig. 4) is not sharp. μ_p^i (μ_{bp}^i) is the chemical potential for interaction between polarons (bipolarons). Using the following charge balance condition

$$x=0.32-2[\mathrm{bp}]-[p] , \tag{8}$$

and combining with Eq. (7), an expression for ΔE^0, the difference in formation potentials, $E_{\mathrm{bp}}^0-E_p^0$, is obtained,

$$\Delta E=\frac{RT}{F}\ln\left[\frac{[p]^2}{0.32[\mathrm{bp}]-2[\mathrm{bp}]^2-[p][\mathrm{bp}]}\right]-\frac{\Delta\mu^i}{F} . \tag{9}$$

The difference in potential, plus any interaction potentials, is also plotted in Fig. 16. Thus, there is a difference of ≈ 0.1 V in the standard potentials, or a difference of ≈ 0.1 eV energy between polaron and a bipolaron, assuming the interaction potentials for both species are the same ($\Delta\mu^i=0$). However, as will be shown below, $\Delta\mu^i$ is not negligible.

The data in Fig. 16 can also be used to rationalize the behavior of the optical spectroscopy. From the EPR data it is clear that polarons and bipolarons coexist at most applied potentials. These data can be used to determine the relative contributions of the two species to the subgap peaks at 1.68 and 0.64 eV. First, the absorbance of the interband peak was measured on a sample of uniform, known thickness deposited on quartz. This value was then used to calibrate the absorbances and thickness of the platinum-mesh supported ultraviolet–visible samples. The molar absorptivity $\varepsilon_{\max,i}$ of the interband transition was found to be 2.9×10^4. Through comparison of the polaron versus V profile in Fig. 16 with the behavior of Fig. 13, it was inferred that polarons were mainly responsible for the band at 1.68 eV. The absorbance values were obtained from a summation of polaron and bipolaron contributions,

$$A=\varepsilon_{1.68,\mathrm{pol}}C_{\mathrm{pol}}L+\varepsilon_{1.68,\mathrm{bipol}}C_{\mathrm{bipol}}L , \tag{10}$$

where $\varepsilon_{1.68}$ are the molar absorptivities at 1.68 eV, C is the molar concentration, and L is the thickness of the film. The concentration is given by $C=7y$, where y is the number of polarons (bipolarons) per repeat unit, and the value of 7 is obtained from the density of PDMPV (1120 $\mathrm{g\,l^{-1}}$) and the molecular weight of a repeat unit (162 $\mathrm{g\,mol^{-1}}$). Values of $\varepsilon_{1.68}$ were chosen to fit the optical data. Figure 13 shows a fit with $\varepsilon_{1.68,\mathrm{pol}}=4.6\times10^5$ and $\varepsilon_{1.68,\mathrm{bipol}}=0$ for charging. Thus it appears that there is very little contribution to the 1.68-eV band from bipolarons.

Since the band at 0.64 eV continues to rise after $3.7V_{\mathrm{applied}}$, it must contain some contribution from bipolarons. Figure 14 shows a fit to Eq. (10) for $\varepsilon_{0.64,\mathrm{bipol}}=1.4\times10^5$ and $\varepsilon_{0.64,\mathrm{pol}}=0$. Better agreement is obtained with some contribution from polarons; for instance $\varepsilon_{0.64,\mathrm{pol}}=2.6\times10^5$ and $\varepsilon_{0.64,\mathrm{bipol}}=6.4\times10^4$ (Fig. 14).

These results show that there is considerably less transfer of oscillator strength from LEP to HEP for bipolarons than for polarons. In fact, the peak at 1.68 eV seems to be derived entirely from polarons. The conclusion is that symmetry breaking by electron-lattice, or other interactions, has *more effect on polarons than on bipolarons.* This result is counterintuitive, since one would expect electron-lattice coupling, or Coulomb correlations, to be more significant for the doubly charged bipolaron. At present we have no explanation for this dilemma.

D. Differences in symmetry breaking

Peak A in Fig. 14 can be associated with polarons and peak B with bipolarons. A similar assignment can be made for peaks A and B in Fig. 1. The reversed relative magnitude of the peaks in the derivative absorption, compared with the peaks in the cyclic voltammogram, can be explained by the fact that polarons have higher molar absorptivity here than biplarons. A straightforward estimate of ΔE^0 can be made by comparing the separation of the peaks in both sets of data (Figs. 1 and 14). The value of ΔE^0 is thus about 0.35 V, or 0.35 eV per defect. Theoretical treatments based on Hückel theory with σ-bond compressibility indicate that the bipolaron binding energy is larger than two polarons by 0.45 eV in polypyrrole[63] and 0.34 eV in polyparaphenylene,[64] which are also examples of polymers with nondegenerate ground states. Calculated differences for PDMPV are expected to be similar. The value of ΔE^0 obtained here can be compared with Eq. (9): $\Delta E^0=-0.1-(\mu_{\mathrm{bp}}^i-\mu_p^i)=0.35$ V. Thus the difference in interaction potentials is 0.45 V. In other words the interaction energy of a polaron is 0.45 eV

greater than a bipolaron, in accordance with the above findings that there is greater symmetry breaking for polarons. The nature of the interaction, be it electron-lattice coupling or Coulombic effects, remains unclear.

E. Excitons and absorptions at higher energies

Referring to Fig. 11, peaks at 3.7 and 4.8 eV decrease with doping. This phenomenon is not explained by the polaron-bipolaron theory or any extension thereof, since the energies involved are much greater than the band gap. Recently, we have successfully applied a combination of molecular-orbital and electron-exciton models to describe the observed electronic absorption spectra of nascent[65] and doped[38] PPV. We have found this approach to be useful for determining absorption bands in the undoped polymer. Semiempirical molecular-orbital–(MO/INDO) calculations on neutral PPV involving all π and σ electrons in four phenylene vinylene units allowed the accurate estimation of the energy and magnitude of absorptions between 3.7 and 6.2 eV due to excitations between localized molecular states. We believe that the absorptions seen in PDMPV at 3.7 and 4.8 eV can also be treated in the same manner. The decrease in intensity of these bands would be due to a transition of the four-repeat-unit molecular state to the quinnoidal geometry of a dication.[38] Two absorptions seen at 0.8 and 2.1 eV that evolve in doped PPV were also accounted for, though with less accuracy. The width and location of the lowest energy absorption at 3.1 eV in neutral PPV, attributed to interband transitions in the polaron-bipolaron model, is also predicted by our vibrationally coupled exciton model. Fine structure seen in this peak at low temperature, due to the vibrational progression which perturbs overlapping exciton states, lends additional weight to an exciton model for this particular band.

V. CONCLUSIONS

The polymer studied here shows regimes of optical, magnetic, and transport behavior that may be correlated using a common voltage axis. In order to analyze the spectroscopic data in terms of the polaron-bipolaron theory, significant symmetry breaking must be invoked. Moreover, polarons and bipolarons appear not to be affected to the same degree by the symmetry breaking, a possibility which has previously not been considered. According to the electrochemical treatment of the results, conducting polymers will invariably have a finite concentration of both polarons and bipolarons. The relative concentrations will depend on the difference in standard formation potentials and interaction energies. The choice of material, PDMPV, was crucial to our ability to make comparisons between material properties. For example, we were unable to carry out the *in situ* conductivity and EPR measurements with PPV, since this polymer exhibited very slow surface-limited doping. While it is possible to rationalize the populations of optical and magnetic species using available polaron-bipolaron models, the magnitude of the conductivity is not explicitly given and depends on sample purity, morphology, and doping methods.

ACKNOWLEDGMENTS

The authors gratefully acknowledge support for this work provided by U.S. Air Force Office of Scientific Research (AFOSR) Grant No. 87-0033.

*Present address: Department of Chemistry and Center for Materials Science Research and Development (MARTECH) Florida State University, Tallahassee, FL 32306.

[1] *Handbook of Conducting Polymers,* edited by T. A. Skotheim (Marcel Dekker, New York, 1986).
[2] J. C. W. Chien, *Polyacetylene: Chemistry, Physics, and Materials Science* (Academic, New York, 1984).
[3] J. R. Reynolds, J. B. Schlenoff, and J. C. W. Chien, J. Electrochem. Soc. **132**, 1131 (1985).
[4] P. Bernier, Mol. Cryst. Liq. Cryst. **83**, 57 (1982).
[5] E. M. Genies, G. Bidan, and A. F. Diaz, J. Electroanal. Chem. **149**, 101 (1983).
[6] A. Feldblum, J. H. Kaufman, S. Etemad, A. J. Heeger, T. C. Chung, and A. G. MacDiarmid, Phys. Rev. B **26**, 815 (1982).
[7] A. J. Epstein, H. Rommelmann, M. Abkowitz, and H. W. Gibson, Phys. Rev. Lett. **47**, 1549 (1981).
[8] J. C. W. Chien, J. M. Warakomski, F. E. Karasz, W. L. Chia, and C. P. Lillya, Phys. Rev. B **28**, 6937 (1983).
[9] J. Chen and A. J. Heeger, Phys. Rev. B **33**, 1990 (1986).
[10] P. Kuivalainen, H. Stubb, P. Raatikainen, and C. Holmstrom, J. Phys. (Paris) Colloq. **44**, C3-757 (1983).
[11] M. J. Nowak, S. D. D. V. Righooputh, S. Hotta, and A. J. Heeger, Macromolecules **20**, 965 (1987).
[12] M. Nechtschein, F. Devreux, F. Genoud, E. Vieil, J. M. Pernaut, and E. Genies, Synth. Met. **15**, 59 (1986).
[13] S. H. Glarum and J. H. Marshall, J. Electrochem. Soc. **134**, 2160 (1987).
[14] J. H. Kaufman, N. Colaneri, J. Scott, and G. B. Street, Phys. Rev. Lett. **53**, 1005 (1984).
[15] F. Genoud, M. Gugliemi, M. Nechtschein, E. Genies, and M. Salmon, Phys. Rev. Lett. **55**, 118 (1985).
[16] H. Holczer, J. P. Boucher, F. Devreux, and M. Nechtschein, Phys. Rev. B **23**, 1051 (1981).
[17] J. L. Bredas and G. B. Street, Acc. Chem. Res. **18**, 309 (1985).
[18] A. J. Heeger, Polym. J. **17**, 201 (1985).
[19] H. S. White, G. P. Kittlesen, and M. S. Wrighton, J. Am. Chem. Soc. **106**, 5375 (1984).
[20] D. R. Gagnon, J. D. Capistran, F. E. Karasz, and R. W. Lenz, Polym. Bull. **12**, 293 (1984).
[21] I. Murase, T. Ohnishi, T. Noguchi, and M. Hirooka, Polym. Commun. **25**, 327 (1984).
[22] R. A. Wessling and R. G. Zimmerman, U.S. Patent No. 3 706 677 (1972).
[23] K. K. Kanazawa, A. F. Diaz, W. D. Gill, P. M. Grant, G. B. Street, G. P. Gardini, and J. F. Kwak, Synth. Met. **1**, 329 (1980).
[24] N. Colaneri, M. Nowak, D. Spiegel, S. Hotta, and A. J. Heeger, Phys. Rev. B **36**, 7964 (1987).
[25] T. Kobayashi, H. Yoneyama, and H. Tamura, J. Electroanal. Chem. **177**, 281 (1984).
[26] D. R. Gagnon, F. E. Karasz, E. L. Thomas, and R. W. Lenz, Synth. Met. **20**, 85 (1987).

[27]T. Granier, E. L. Thomas, D. R. Gagnon, F. E. Karasz, R. W. Lenz, J. Polym. Soc. Polym. Phys. Ed. **24**, 2793 (1986).
[28]J. L. Brédas, Ref. 1.
[29]J. M. Machado, J. B. Schlenoff, and F. E. Karasz, Macromolecules **22**, 1964 (1989).
[30]C. C. Han, R. W. Lenz, and F. E. Karasz, Polym. Commun. **28**, 261 (1987).
[31]S. Antoun, F. E. Karasz, R. W. Lenz, J. Polym. Sci. Pt. A **26**, 1809 (1988).
[32]J. B. Schlenoff, J. M. Machado, P. J. Glatkowski, F. E. Karasz, J. Polym. Sci. Pt. B **26**, 2247 (1988).
[33]K. Y. Jen, L. W. Shacklette, and R. Elsenbaumer, Synth. Met. **22**, 179 (1987).
[34]K. Kaneto, M. Maxfield, D. P. Nairns, A. G. MacDiarmid, and A. J. Heeger, J. Chem. Soc. Farad. Trans. I **78**, 3417 (1982).
[35]L. W. Shacklette and J. E. Toth, Phys. Rev. B **32**, 5982 (1985).
[36]J. H. Kaufman, T. C. Chung, and A. J. Heeger, J. Electrochem. Soc. **131**, 2847 (1984).
[37]G. P. Kittlesen, H. S. White, and M. S. Wrighton, J. Am. Chem. Soc. **106**, 7389 (1984).
[38]J. Obrzut and F. E. Karasz, J. Chem. Phys. **87**, 6178 (1987).
[39]J. B. Schlenoff and J. C. W. Chien, Synth. Met. **22**, 348 (1988).
[40]J. C. W. Chien and J. B. Schlenoff, Nature (London) **311**, 362 (1984).
[41]T. Kobayashi, H. Yoneyama, and H. Tamura, J. Electroanal. Chem. **177**, 293 (1984).
[42]A. F. Diaz, J. I. Castillo, J. A. Logan, and W. Y. Lee, J. Electroanal. Chem. **129**, 115 (1981).
[43]G. Ahlgren, B. Krische, A. Pron, and M. Zagorska, J. Polym. Sci. Polym. Lett. Ed. **22**, 173 (1984).
[44]E. W. Paul, A. J. Ricco, and M. S. Wrighton, J. Phys. Chem. **89**, 1441 (1985).
[45]K. J. Wynne and G. B. Street, Macromolecules **18**, 2361 (1985).
[46]M. J. Obrzut and F. E. Karasz, Macromolecules **22**, 458 (1989).
[47]A. J. Epstein, Ref. 1.
[48]I. G. Austin and N. F. Mott, Adv. Phys. **18**, 41 (1969).
[49]J. M. Saveant, J. Phys. Chem. **92**, 1011 (1988).
[50]J. M. Madsen, B. R. Johnson, X. L. Hua, R. B. Hallock, M. A. Masse, F. E. Karasz, Phys. Rev. B **40**, 11 751 (1989).
[51]K. Soga and M. Nakamura, J. Chem. Soc. Chem. Commun. 1495 (1983).
[52]E. E. Havinga and L. W. Van Horssen, Synth. Met. **16**, 55 (1986).
[53]K. D. Gourley, C. P. Lillya, J. R. Reynolds, and J. C. W. Chien, Macromolecules **17**, 1025 (1984).
[54]S. A. Brazovski and N. Kirova, Pis'ma Zh. Eksp. Teor. Fiz. **33**, 6 (1981) [JETP Lett. **33**, 4 (1981)].
[55]H. Takayama, Y. R. Lin-Lin, and K. Maki, Phys. Rev. B **21**, 2388 (1980).
[56]W.-P. Su, J. R. Schrieffer, and A. J. Heeger, Phys. Rev. Lett. **42**, 1698 (1979).
[57]K. Fesser, A. R. Bishop, and D. K. Campbell, Phys. Rev. B **27**, 4804 (1983).
[58]D. Bertho and C. Jouanin, Synth. Met. **24**, 179 (1988).
[59]U. Sum, K. Fesser, and H. Büttner, Phys. Rev. B **38**, 6166 (1988).
[60]D. Baeriswyl and K. Maki, Phys. Rev. B **31**, 6633 (1985).
[61]J. E. Hirsch, Phys. Rev. Lett. **49**, 1455 (1982).
[62]M. J. Rice and E. J. Mele, Phys. Rev. Lett. **49**, 1455 (1982).
[63]J. L. Bredas, J. C. Scott, K. Yakushi, and G. B. Street, Phys. Rev. B **30**, 1023 (1984).
[64]J. L. Bredas, R. R. Chance, and R. Silbey, Mol. Cryst. Liq. Cryst. **77**, 319 (1981).
[65]J. Obrzut and F. E. Karasz, J. Chem. Phys. **87**, 2349 (1987).